Subharmonic frequency locking in the resistive Josephson thermometer

M. van Veldhuizen

Department of Mathematics and Computer Science, Free University, De Boelelaan 1081, 1081 HV Amsterdam, The Netherlands

H. A. Fowler

Center for Applied Mathematics, National Bureau of Standards, Gaithersburg, Maryland 20899

Phase-locked oscillatory solutions are examined as a basis for the dc impedance of the resistive superconducting quantum-interference device Josephson thermometer. The calculations are based on the resistively shunted junction model in the limit $2\pi L_s I_c/\Phi_0 \geq 1$, where L_s is the loop inductance and I_c is the junction critical current, and for a junction resistance large compared with the external shunt resistance. An algorithm for representing frequency entrainment in (κ, ω) space (drive amplitude, frequency) leads to zones with rotation number p/q having the form of leaf-shaped regions joined and overlapping at their tips. High-resonance zones are very thin and locally similar. No chaotic behavior has been observed. The model can simulate the "rising" curves of dc impedance as a function of drive amplitude.

INTRODUCTION

In a series of experiments carried out by Soulen and Giffard[1] and by van Vechten et al.[2] it was found that the dc impedance of a resistive superconducting quantum interference device (SQUID) is a very complicated function of the SQUID parameters. Much analytical work has been done in order to describe this dependence; see Soulen and Giffard,[1] Peterson,[3] Wiesenfeld et al.,[4] and Sanders.[5] Here we put forward a new form of parameter-space representation, relating the measured data to high-resonance frequency-locked solutions of the mathematical model for the resistive SQUID. The frequency-entrainment zones in (κ, ω) space display a characteristic form consisting of overlapping leaf-shaped regions. High-resonance zones turn out to be very thin. In addition, these thin zones are similiar in shape, at least locally. By means of the numerically observed similarity in shape we are able to relate the profile of the zones to the measured data for the dc impedance (see Soulen and Giffard[1]).

DEFINITION OF RESONANCE ZONES

We consider a rf-biased resistive SQUID consisting of a SQUID ring and a tank circuit (see Soulen and Giffard[1] and Wiesenfeld et al.[4]). The SQUID ring is characterized by a Josephson junction, an inductance L_s, and a small resistor R. A dc bias current I_0 is fed through the resistor R. The Josephson junction is characterized by the Josephson relations

$$V_J = \frac{\Phi_0}{2\pi}\dot{\phi}, \quad I_J = I_c \sin\phi ,$$

where V_J is the voltage across the junction, ϕ the quantum-mechanical phase difference across the junction, I_c its critical current, I_J the current through the junction, and Φ_0 the flux quantum. The capacitance of the Joseph-

son device (a point contact) is neglected because of the small surface area involved. With a mutual induction M between the tank circuit and the SQUID ring and an ac current $I_{rf}\sin(\Omega t)$ in the tank circuit, we arrive at the following differential equation for the phase difference ϕ across the junction:

$$\beta\ddot{\phi} + (1 + \gamma\cos\phi)\dot{\phi} = \alpha - \sin\phi + \kappa\omega\cos(\omega t + 2\pi\eta) , \quad (1)$$

where time has been rescaled so that $t = \omega_c t_{old}$,

$$\omega_c = \frac{2\pi R I_c}{\Phi_0}, \quad \omega = \frac{\Omega}{\omega_c} ,$$

$$\alpha = \frac{I_0}{I_c}, \quad \beta = \frac{\omega_c L_s}{R_j}, \quad \gamma = \frac{\omega_c L_s}{R} ,$$

with κ proportional to M and I_{rf} (see Wiesenfeld et al.[4]). R_j is the zero-voltage (subgap) limit of the tunneling resistance for the Josephson point contact. γ thus defined represents only the inductive back-emf reflected from the external inductance L_s, and does not include consideration of the coherent normal current in the point contact. Typical values are $\omega \simeq 250-10\,000$, $\beta \simeq 10^{-5}$, and $\gamma \simeq 1.0$. By a $p:q$ resonance solution of the driven Josephson equation (1) we denote a solution ϕ such that

$$\phi\left[p\frac{2\pi}{\omega}\right] = \phi(0) + 2\pi q , \quad (2a)$$

$$\dot{\phi}\left[p\frac{2\pi}{\omega}\right] = \dot{\phi}(0) . \quad (2b)$$

We always assume p and q to be relatively prime. Values of $\phi(t)$, $\dot{\phi}(t)$ are computed approximately by integrating the differential equation (1) using an adaptive numerical-integration routine. To obtain a $p:q$ resonance solution, (2a) and (2b) are then solved by successive linearizations (Newton's method in combination with a so-called simple

shooting method, using partial derivatives as calculated in the adaptive integration). In view of the jumps and dips in the solution, extreme accuracy is called for. Tolerances of 10^{-9} or less have been used. The external phase η is introduced as a numerical convenience, so that the initial value $\phi(0)$ may be set at a common fixed value in a region where the solution is particularly smooth. Therefore, we put $\phi(0) = \phi_0$, a prescribed value. The two unknowns in (2a) and (2b) are then $\dot{\phi}(0)$ and one of the parameters α, β, γ, κ, ω, or η; all other parameters must be prescribed.

Observe that a $p:q$ resonance solution ϕ is frequency locked with respect to the external ac frequency ω in that

$$\langle \dot{\phi} \rangle = \lim_{T \to \infty} \frac{\phi(T) - \phi(0)}{T} = \frac{q}{p} \omega , \quad (3)$$

where $\langle \dot{\phi} \rangle$ is the dc-averaged voltage used for representing the dc impedance of the resistive SQUID thermometer.

If η is varied between 0 and 1, a region of solutions is found in (κ, ω) space; it is bounded by maximum and minimum values in ω for any fixed value of κ. If we plot the set of all pairs (κ, ω) for which a $p:q$ resonance solution exists, we find that it depends on the value of the parameters α, β, and γ, but not the phase shift η nor on the prescribed value of $\phi(0)$. This bounded region of stable resonances in the (κ, ω) plane is called a *p:q resonance* or *entrainment zone*, resembling in shape a branch of a cactus plant. By defining a resonance zone as a set in the (κ, ω) plane the underlying idea of frequency resonance is emphasized.

As an example of an entrainment zone in the (κ, ω) plane consider the 7:2 resonance zone shown in Fig. 1. The root of the zone is at $\omega = 37.6943$, at $\frac{7}{2}$ times the frequency of the autonomous system. The striking shape is immediately evident. The leaves numbered A, B, ... are regions of subharmonic frequency entrainment in (κ, ω) space, within which a stable (and an unstable) frequency-locked solution of specified $p:q$ resonance are found. Where the tips of the leaves overlap, two stable $p:q$ resonance solutions can be found; these are distinguished by a different content of higher harmonics. At the borders the stable solution and the unstable one coincide. Outside these boundaries no $p:q$ resonant solutions are found. The oscillatory character of the 7:2 resonance solutions increases at each new leaf. The overlapping tips of the leaves correspond to the inclusion of successively higher harmonics of the drive frequency in the Fourier content of the solution as κ increases. In crossing the "jump" regions where $1 + \gamma \cos(\phi) < 0$, $\dot{\phi}$ rises to high values (voltage spikes) during a cycle of the drive voltage $\cos(\omega t)$. The number of these spikes encountered during a drive cycle increases with κ. The subharmonic selection criteria (2a) and (2b) permit solutions of this type, since they do not discriminate against aliasing. In view of its definition no period-doubling effect takes place in the $p:q$ entrainment zone. In the parameter regions we have examined, as κ is increased, the system evidently absorbs more drive energy in the form of higher harmonics of the drive frequency, rather than in period-doubling subharmonics of the relaxation limit cycle or the drive cycle. This has been checked by plotting solutions at a number of cuts through
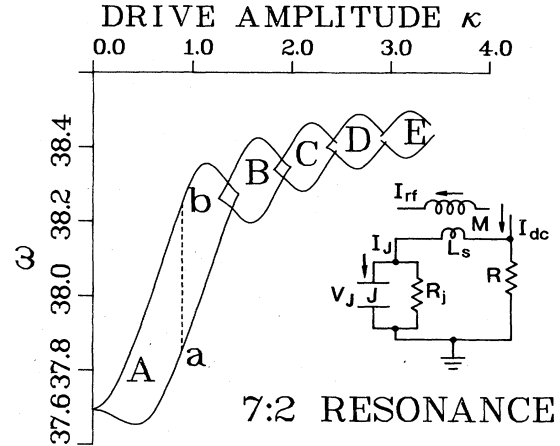

FIG. 1. The 7:2 resonance zone for $\alpha = 11$, $\beta = 0.01$, and $\gamma = 1.5$. Within each lettered region denoted $A, B, \ldots$ there exists at least one pair of frequency-locked solutions with winding number $\frac{7}{2}$, one stable, one unstable. At the border of the leaf-shaped regions the stable and the unstable ones meet. The line a-b for $\kappa = 0.9$ is the set of solutions displayed on the 7:2 resonance line in Fig. 2. Although the zone commences for small κ, in the manner of Arnold's regions of resonance (Ref. 10), its form for larger κ is distinctly different. The horizontal axis is in units of RI_c (rf voltage amplitude); the vertical axis is in units of ω_c. Inset illustrates the resistive SQUID loop.

the branches. In addition, a search for a 14:4 resonance solution at higher κ values did not result in new solutions. Thus, the case (1) seems to have characteristics different from the model considered by Goldhirsch et al.[6] and Octavio[7] where $\beta \simeq 1$ and $\gamma = 0$.

Alternative definitions are possible. For instance, one obtains analogous leaves in the physically relevant (α, κ) plane by interchanging the role of ω and α in the above definition. However, the underlying idea of resonance is obscured in such definitions. On the other hand, one now obtains the well-known Shapiro[8] steps in the $(\alpha, \langle \dot{\phi} \rangle)$ characteristics. The width of a zone at height κ corresponds to the size of the step. For some work and ideas on the size of such steps see Allen.[9] However, our zones seem thinner than the prediction of Allen,[9] which describes a simpler model of locking.

RESONANCE ZONES AND $\langle \dot{\phi} \rangle$

For any resonance solution ϕ in a $p:q$ entrainment zone formula (3) relates $\langle \dot{\phi} \rangle$ and its computation to the resonance-zone patterns.

First, we might use these resonance zones to obtain values of $\langle \dot{\phi} \rangle$ as a function of κ, using (3) directly. The computation, which is already complex for moderate values of p, becomes increasingly laborious at higher values when high precision is sought in evaluating $\langle \dot{\phi} \rangle$. At a minimum, the differential equation must be integrated three or four times between $t = 0$ and $t = 2\pi p / \omega$ (the number of Newton iterations with an approximate Jacobian matrix).

Second, one might compute $\langle \dot{\phi} \rangle$ by averaging a numer-

ical solution. In this case one integrates ϕ from $t=0$ up to some value $t=T$, approximating ϕ on $[0, T]$ in the least-squares sense by a linear function. The slope of this straight line is the approximation to $\langle \dot{\phi} \rangle$. Clearly, if we perform this process for a point in the parameter space corresponding to a $p:q$ resonance solution, then the length T of the integration interval must be at least as large as the period $2\pi p / \omega$ of the $p:q$ resonance solution. If not, one simply overlooks part of the solution and the result may be incorrect. In practice, the length of the integration interval should be a multiple (at least 10, and often a higher multiple) of the period $2\pi p / \omega$.

If Fig. 1 were extended to higher values of ω, we would find additional zones corresponding to the rational-number subharmonics; these would appear above the 7:2

resonance zone. This spectrum of resonances may be calculated instead by the least-squares averaging procedure.

As an example consider the computation by this algorithm of $\langle \dot{\phi} \rangle$ for the model (1) with $\alpha = 11.0$, $\beta = 0.01$, $\gamma = 1.5$, and $\kappa = 0.9$. Since the ratio $\langle \dot{\phi} \rangle / \alpha$ is commonly defined as the "dc impedance" of the device, we give the results for $\langle \dot{\phi} \rangle / \alpha$ in Fig. 2. Where the line $\kappa = 0.9$ in the (κ, ω) plane intersects a leaf zone we find a linear-slope region as a consequence of relation (3). Hence, by computing the points where the border of a leaf zone intersects the line $\kappa = 0.9$, an independent check on the zone width is possible from comparison with this averaging procedure. This has been done for four linear-slope regions as indicated in Fig. 2. In particular, the 7:2 resonance zone and the line $\kappa = 0.9$ have the segment a-b as intersection, cf.
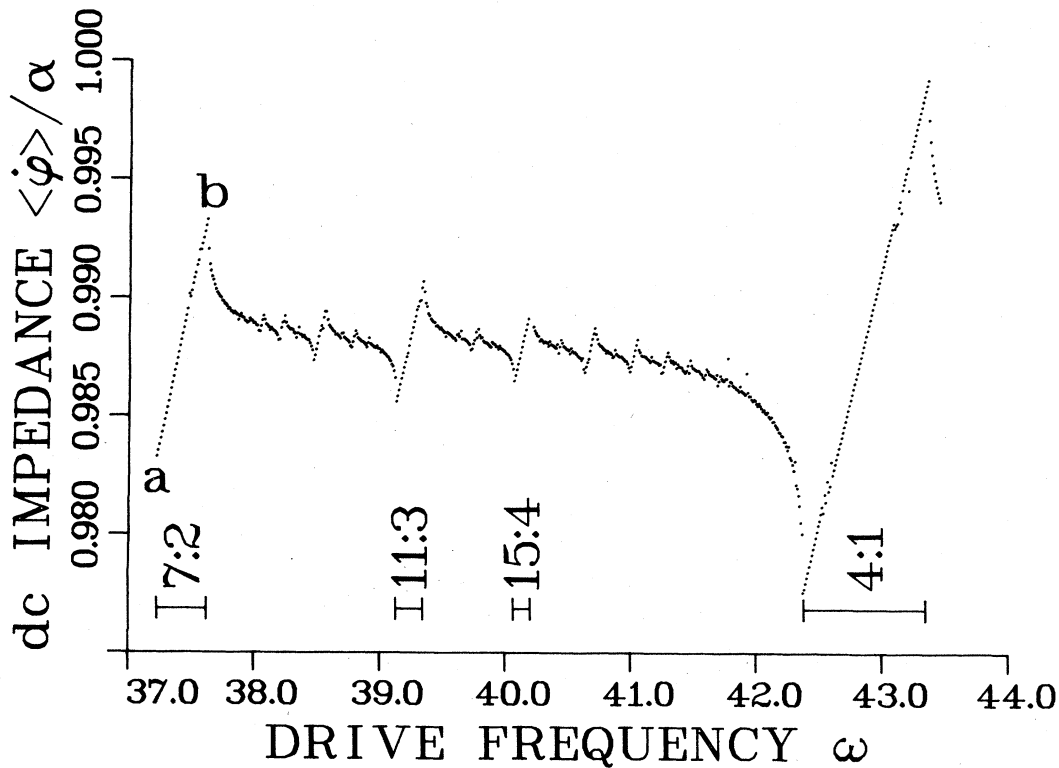

FIG. 2. dc impedance $\langle \dot{\phi} \rangle / \alpha$ vs ω for (1) with $\alpha = 11$, $\beta = 0.01$, $\gamma = 1.5$ with $\kappa = 0.9$. The value of $\langle \dot{\phi} \rangle$ is computed as the slope of a linear least-squares approximation to a solution. Some resonance zones are indicated, many others are visible. At intersections with zones the linear relation (3) must hold true (linear-slope regions). This gives some impression about the possible numerical error in the computations. Note that a-b shows the same set of 7:2 solutions that are indicated on the resonance zone in Fig. 1. In fact, this plot approximates the rotation number as a function of ω. Note the characteristic infinite slope at the end of the phase-locked regions. In the curved (non-phase-locked) parts of the plot, the linear average of the $\langle \dot{\phi} \rangle$ solution to (1) is computed after a "run-in" period, to eliminate transients; the rotation number is *not* assumed rational in the averaging procedure. The horizontal axis is in units of ω_c; the vertical axis is in units of R.

Figs. 1 and 2. Each of the linear-slope regions in Fig. 2 corresponds to a subharmonic Shapiro step in the $(\alpha, \langle \dot{\phi} \rangle)$ plane, i.e., in the I-V characteristic curve of the system, as it would be "seen" with a sweep of the drive frequency.

The deviations in the linear-slope regions, e.g., in the 4:1 resonance zone, are due to numerical noise (truncation at time T, accumulation of errors on the rather long integration interval). This has been checked explicitly for a few cases. The computational results suggest a width of a p:q zone proportional to $(P + q)^{-3/2}$.

The sample shown in Fig. 2 approximates the rotation number of a flow as a function of ω. As such it shows the typical behavior at the ends of the phase-locked regions (the linear-slope regions), where it takes off with an infinite derivative. A simple example showing the same characteristics is discussed by Guckenheimer and Holmes.[10]

The conclusion seems to be that the approximation of $\langle \dot{\phi} \rangle$ in the neighborhood of a p:q resonance solution with large p is necessarily expensive with both algorithms described above. In most cases the computation will be too expensive. Asymptotic formulas might offer a useful alternative, but the existing asymptotic results of Sanders[5] for $\langle \dot{\phi} \rangle$ have not been proved to be valid for $\gamma > 1$. Here we emphasize that the existence of the leaf-shaped zones is not restricted to $\gamma > 1$. Later we shall give an example for $\gamma = 0.8$.

It is not known either whether an arbitrary solution tends toward a resonance solution as time tends toward infinity. In any case, numerical experiments suggest that this is indeed the case, but numerical evidence cannot be conclusive in this case.

SIMILARITY OF RESONANCE ZONES

Roughly speaking a solution ϕ of the differential equation (1) grows like αt. Hence, for a p:q resonance solution we have approximately

$$\frac{p}{q} \simeq \frac{\omega}{\alpha} . \tag{4}$$

With $\omega = 4000.0$ and $\alpha = 2.0$ we arrive at $p/q = 2000$. Such values of p/q are too large for performing numerical experiments on even a minor scale. Consequently, numerical experiments have been performed for values of p/q up to 400. We choose $\gamma > 1$, because the asymptotic formulas of Sanders[5] cover the case $\gamma < 1$ already.

The experiments suggest the following conclusions:

(1) The p:q resonance zones for large p/q are very *thin* indeed. In one experiment, the width of a 400:1 resonance zone is approximately 10^{-8} relative to the resonance frequency 3080.0. The accuracy in the numerical approximations is only slightly better.

(2) Locally in p/q numerical results satisfy in good precision

$$\frac{q}{p} \omega_{p:q}(\kappa, \eta) \simeq \mu(\kappa) , \tag{5}$$

where p/q is large. Here $\omega_{p:q}(\kappa, \eta)$ denotes the resonance frequency of the p:q resonance solution for the parameters κ and η. The function μ depends neither on p, nor q,
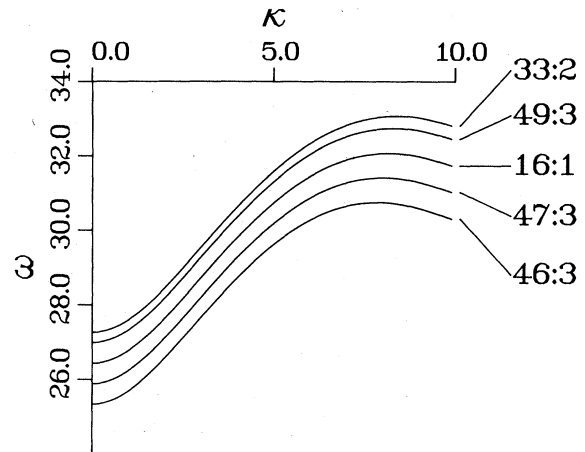

FIG. 3. Five resonance zones are drawn in one figure as indicated for $\alpha = 2$, $\beta = 0.1$, and $\gamma = 1.02$. The similarity in form is obvious in this case. Usually, the 16:1 resonance zones are already threadlike. Note that these are not curves, but regions of finite width; however, they are so thin that they can only be represented by curves. Axis units are as in Fig. 1.

nor η, at least for p/q large, but it does depend on α, β, and γ. Of course, for $\kappa = 0$ the relation (5) holds true exactly. Since for p/q large the entrainment regions are so thin this relation implies that all high-resonance zones are *similar in shape*, at least locally. An example is given in Fig. 3, where a 16:1, a 33:2, a 49:3, a 47:3, and a 46:3 resonance zone are drawn in one figure. The similarity is obvious in this case. The relation (5) has been checked numerically for several sets of parameter values. The similarity relation (5) suggests that the set of all high-resonance entrainment zones is locally a dense set.

(3) There seems to be *no chaotic behavior* of solutions of (1) in the parameter region covered. Indeed, chaotic behavior would imply intersection of zones and vice versa, contradicting the similarity property stated above. In this respect Eq. (1) behaves differently from the one considered by (among others) Goldhirsch et al.[6] and Octavio.[7]

A CONSEQUENCE OF THE SIMILARITY OF THE RESONANCE ZONES

We now use two tentative conclusions from the preceding section—very thin resonance zones, and similarity in form—as assumptions in order to relate these zones to measured data for $\langle \dot{\phi} \rangle$. Suppose we ask for the value of $\langle \dot{\phi} \rangle$ along the line $\omega = \omega_{rf} = $ constant. In view of (3) we know the value of $\langle \dot{\phi} \rangle$ along this vertical line at intersections with resonance zones. A physically plausible model describes a solution as one that stays on a resonance curve for a considerable time before it is perturbed to a neighboring (stable) curve of nearly indistinguishable form. So suppose $\langle \dot{\phi} \rangle_\kappa$ is given. Then, because the solution stays for a long time on a p_κ:q_κ resonance solution, we have in view of (3)

$$\frac{q_\kappa}{p_\kappa}\omega_{\text{rf}}=\langle\dot\phi\rangle_\kappa. \tag{6}$$

On the other hand, the similarity in form of the zones implies

$$\langle\dot\phi\rangle_\kappa=\frac{q}{p}\omega_{p:q}(\kappa,\eta) \tag{7}$$

for any pair p,q in the neighborhood of p_κ,q_κ. Here we use the fact that the function μ in (5) depends only on κ and not on η, p, and q. Thus, points $\omega_{p:q}(\kappa,\eta)$ in the $p:q$ resonance zone are related to measured data $\langle\dot\phi\rangle_\kappa$ at the frequency ω_{rf} by (7). In fact, *what this says is that the curves measured by Soulen and Giffard[1] may be interpreted as high-resonance zones.*

Unfortunately, the computation of these entrainment zones is a rather delicate one, because each point in the zone requires solving the two highly nonlinear equations (2a) and (2b) through an accurate numerical integration of the second-order equation (1). For high-resonance zones some simplifications are possible; the width of the leaf zone is such that one value of η suffices, i.e., no intersection through the zone is necessary. Furthermore, if one
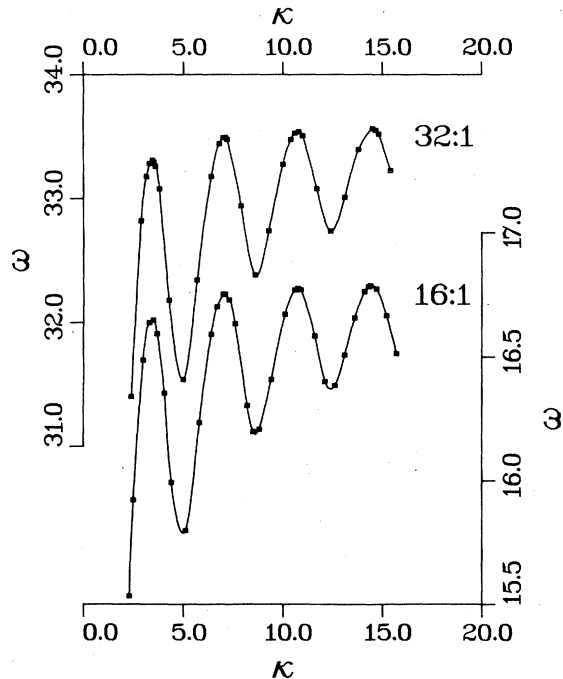
wants to compute points in a (say) $2p:q$ resonance zone, it is often feasible to start with points in a $p:q$ zone. The points in the (ω,κ) plane so obtained can be used as good initial guesses for points in the $2p:q$ zone after multiplication of ω by a factor 2. This kind of similarity relation is usually too inaccurate for direct use, but for numerical use it works fine. An example of this kind of similarity is given in Fig. 4, where a 16:1 and a 32:1 resonance zone are shown.

The disadvantage of analytical methods for relating $\langle\dot\phi\rangle$ to the rf-driving amplitude κ is their restricted scope in parameter space. Most analytical and asymptotic formulas are not valid for $|\gamma|>1$, and points in parameter space with $\beta\omega\simeq1$ are also difficult to handle by analytical methods. Here the new interpretation by means of the overlapping leaf zones comes in. By means of the zone-defining algorithm explained above it is possible to overcome certain restrictions of the analytical and asymptotic methods. This suggests the use of the method primarily for $|\gamma|>1$ and/or $\beta\omega\simeq1$. For $\beta\omega\simeq1$ interesting zone profiles have been found, even if the values of both β and $1/\omega$ are rather large. See Fig. 4 for two profiles showing a "rising" impedance envelope as a function of the rf-driving amplitude κ on the basis of the model (1). Behavior with varying α is illustrated in Fig. 5. For $\gamma=0.8$ (Fig. 6) we find a zone profile corresponding in
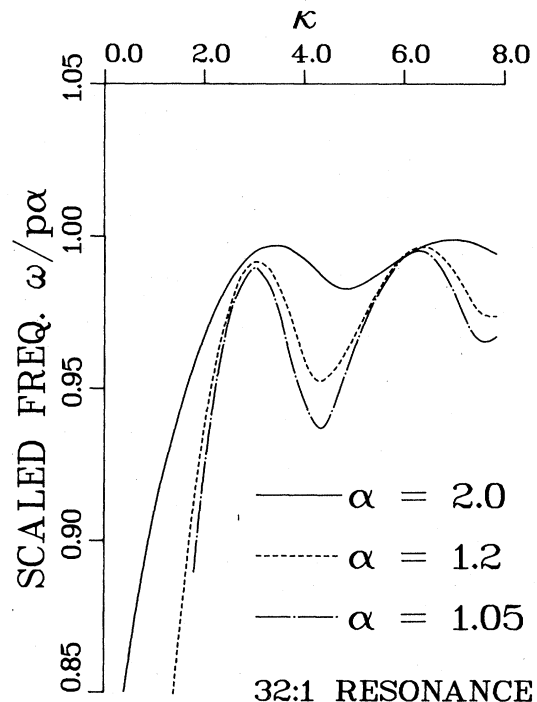

FIG. 4. The 32:1 resonance zone ($\alpha=1.05$, $\beta=0.02$, $\gamma=1.5$) and the 16:1 resonance zone ($\alpha=1.05$, $\beta=0.04$, $\gamma=1.5$) are almost identical. There is a slight deviation for $\kappa>12$. The rising character of both curves is probably due to the particular range of values of $\beta\omega$. Recall that some experimental results of Soulen and Giffard[1] show a similar rising curve. The "rising" envelope described in this calculation originates entirely within the resistive SQUID loop, for a uniform sine-wave driving signal. (Feedback to the drive circuit is excluded.) Note how the progression from $\beta=0.1$ in Fig. 3 to $\beta=0.02$ here is associated with "resolving" additional structure in the κ variations. Axis units are as in Fig. 1.

FIG. 5. Three 32:1 resonance zones, all three of them with $\beta=0.01$, $\gamma=1.5$. The value of α differs as indicated. The scaled frequency on the vertical axis is defined for each $p:q$ resonance zone as $\omega/(p\alpha)$. For $\kappa\simeq6.0$ the zones with $\alpha=2.0$ and $\alpha=1.05$ touch, whereas the one with $\alpha=1.2$ intersects them. The horizontal axis units are as in Fig. 2. The vertical axis now displays $\omega/p\alpha$, instead of ω/α, in units of RI_c (dc voltage).
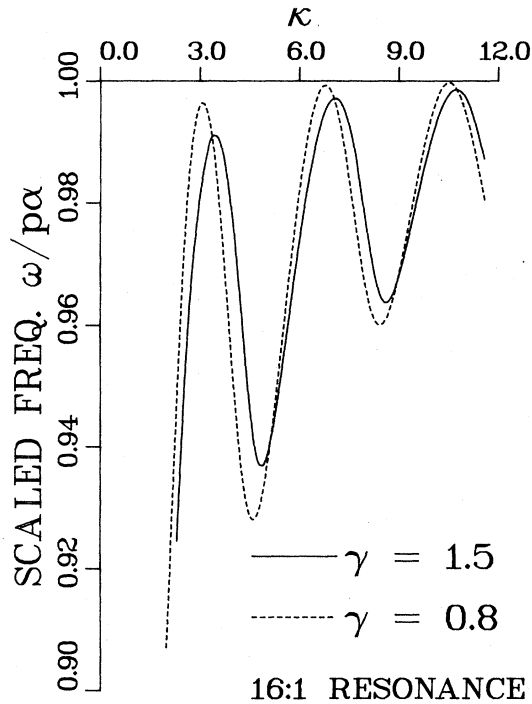
FIG. 6. Two 16:1 resonance zones with $\alpha = 1.05$, $\beta = 0.04$, and $\gamma = 0.8$ and 1.5 as indicated. The resonance zone with $\gamma = 1.5$ also occurs in Fig. 4. The profile is pushed outward in κ for the higher value of γ, and its maxima display a more "rising" character. Axis units are as in Fig. 5.

shape with the asymptotic results of Sanders.[5] The "rising" envelope described by this calculation originates entirely within the resistive SQUID loop, for a uniform sine-wave drive signal. It is separate from any feedback to the Q-resonant circuit which supplies the drive signal. Such feedback has been modeled asymptotically in first order by Seppä[11] for the case $\gamma = 0.5$, in order to simulate a weak inversion from rising to falling envelopes, which is observed [cf. (2)] in crossing the LCR resonance of the driving tank circuit. For $|\gamma|$ large, up to $\gamma = 8$ no zone shapes of special interest have been found. It must be said that the computations for such high values of γ are quite expensive, as is to be expected.

SUMMARY

The $p : q$ resonance zones, which are defined wholly by straightforward numerical procedures, display striking characteristic leaflike shapes which compress rapidly at higher p/q ratios. These extremely thin zones in (κ, ω) space are locally similar, and conform in shape to experimentally observed dependencies of dc impedance $\langle \phi \rangle / \alpha$ on the driving amplitude κ.

The new interpretation by means of resonance zones overcomes the restricted scope of analytical and asymptotic methods in parameter space. It succeeds in identifying and tracking properties of phase-locked solutions in the "difficult" parameter region for $|\gamma| > 1$.

ACKNOWLEDGMENTS

[1]R. J. Soulen, Jr. and R. P. Giffard, Appl. Phys. Lett. **32**, 770 (1978).

[2]D. van Vechten, R. J. Soulen, Jr., and R. L. Peterson, in *Proceedings of the Second International Conference on Superconducting Quantum Interference Devices (SQUID 80)*, edited by H. D. Hahlbohm and H. Lübbig (De Gruyter, Berlin/New York, 1980), p. 569.

[3]R. L. Peterson, J. Appl. Phys. **52**, 7321 (1981).

[4]K. Wiesenfeld, E. Knobloch, R. F. Miracky, and J. Clarke, Phys. Rev. A **29**, 2102 (1984).

[5]J. Sanders, Lect. Notes Math. **985**, 288 (1983).

[6]I. Goldhirsch, Y. Imry, G. Wasserman, and E. Ben-Jacob, Phys. Rev. B **29**, 1218 (1984).

[7]M. Octavio, Phys. Rev. B **29**, 1231 (1984).

[8]S. Shapiro, Phys. Rev. Lett. **11**, 80 (1963).

[9]T. Allen, IEEE Trans. Circuits Syst. **CAS-30**, 627 (1983).

[10]J. Guckenheimer and P. Holmes, *Nonlinear Oscillations, Dynamical Systems and Bifurcation of Vector Fields* (Springer, New York, 1983), especially pp. 298–300.

[11]H. Seppä, J. Appl. Phys. **55(6)**, 1572 (1984).